Effective conductivity due to continuous polarization reorientation in fluid ferroelectrics

Yongqiang Shen,[1] Tao Gong,[2] Renfan Shao,[1] Eva Korblova,[2] Joseph E. Maclennan,[1] David M. Walba,[2] and Noel A. Clark[1,*]

[1]*Department of Physics, Liquid Crystal Materials Research Center, University of Colorado, Boulder, Colorado, 80309, USA*

[2]*Department of Chemistry and Biochemistry, Liquid Crystal Materials Research Center, University of Colorado, Boulder, Colorado, 80309, USA*

A smectic-A (SmA) liquid crystal phase of fluid layers with in-plane polarization **P** is shown to exhibit effective conductivity in the semiconducting range during electric-field-induced polarization reorientation, but becomes insulating once the polarization is aligned with the field. Such fluid ferroelectrics sandwiched between highly insulating layers enable electro-optic devices with long-term dc electrostatic control of polarization and optic axis orientation.

In crystal ferroelectrics, the macroscopic polarization density **P** is stabilized to a set of discrete orientations by the underlying lattice and ferroelectricity characterized by field-induced switching of **P** between these stable states. The electric current accompanying the reversal of **P** arises, in this case, from the motion of domain boundaries [1]. Fluid ferroelectrics exhibit a macroscopic polarization density with no energy barriers to its reorientation. As a result, the polarization can respond to the applied electric field in a continuous fashion, limited only by viscous dissipation. We show here that, due to the reorientation of **P**, an otherwise insulating fluid ferroelectric behaves electrically as a resistive medium, with conductivity in the semiconducting range in a typical mesogenic material.

The known fluid ferroelectrics, chiral smectic-C (SmC) [2] liquid crystals (LCs), and ferroelectric phases of bent-core mesogens [3,4] are phases that have fluid layers and **P** parallel to the layer plane, with no barriers to reorientation [2,5]. In these materials, electrostatic interactions become dominant, especially for large P, with suppression of polarization splay minimizing the generation of polarization charge $\rho_b = -\nabla \cdot \mathbf{P}$ and rendering $\mathbf{P}(r)$ spatially uniform and free to reorient as a homogeneous block [6–9]. When a voltage V is applied between the planar electrodes of a LC cell of area A, generating an electric field **E** as shown in Fig. 1, the equilibrium **P** orients either parallel to the applied field (along $\phi = \pi$) or, if the interfacial capacitance C_I of the cell is sufficiently large, at an angle $\phi(V) = \cos^{-1}(C_I V / P A)$, the orientation at which the free charge and the polarization surface charge cancel to give $E = 0$ in the LC [6]. The latter case is particularly interesting for light control applications since the continuous reorientability of **P** can be exploited to obtain analog electro-optic behavior. In this Rapid Communication we explore the electrodynamics of continuously reorienting high-polarization LCs, showing that rotational viscosity makes their effective impedance resistive, in the semiconducting regime. Measurements of cell dynamics are reported for the Sm$A P_F$ material W623, shown in Fig. 1(a), a bent-core system with high polarization that we find to exhibit nearly ideal field-induced block reorientation of **P**.

The experimental cell geometry is sketched in Fig. 1(b). The LC is a smectic monodomain of thickness d_{LC} oriented with bookshelf geometry between glass plates coated first with indium tin oxide (ITO) electrodes and then with insulating alignment layers of dielectric constant ϵ_I and thickness d_I, as in Fig. 1(c). The layer normal **z** and molecular long axis **n** are oriented parallel to the glass plates. The polarization is perpendicular to the director and reorients around the molecular long axis when an electric field is applied between the electrodes. The two insulating layers are electrically equivalent to a capacitor $C_I = \epsilon_I A / 2 d_I$, as indicated in the equivalent circuit of Fig. 1(d). In the absence of polarization reorientation (for example, when $\phi = 0$ or π and the polarization does not respond to further changes in applied field), the LC layer is insulating, with an equivalent capacitance $C_{\text{LC}} = \epsilon_{\text{LC}} A / d_{\text{LC}}$, where ϵ_{LC} is the dielectric constant and d_{LC} is the thickness of the LC layer. The electrode voltage $V = V_I + V_{\text{LC}}$ and the current through the cell is $i = i_I = i_C + i_P$, where i_C and i_P represent the capacitive and polarization components of current in the LC. Under dynamic driving conditions, the electric field E_{LC} within the liquid crystal is in general nonzero, resulting in a torque on **P** that, when the damping effect of orientational viscosity γ is included, gives the equation of motion [10]

$$\gamma \frac{d\phi}{dt} = P \frac{V_{\text{LC}}}{d_{\text{LC}}} \sin \phi . \tag{1}$$

The polarization current associated with reorientation of **P** is $i_P = A(-d P_x / dt) = A P \sin \phi (d\phi / dt)$. Using Eq. (1) to eliminate $d\phi / dt$ from this expression gives

$$i_P = \frac{A V_{\text{LC}} P^2 \sin^2 \phi}{\gamma d_{\text{LC}}} = \frac{V_{\text{LC}}}{R_P(\phi)} , \tag{2}$$

where $R_P(\phi) \equiv \gamma d_{\text{LC}} / A[P^2 - P_x^2(\phi)] = \gamma d_{\text{LC}} / A(P^2 - P^2 \cos^2 \phi)$ is the effective resistance of the LC. $R_P(\phi)$ depends on the orientation of **P** and is smallest when $P_x(\phi) = 0$ (when $\phi = \pi/2$), where the electrical torque has the largest magnitude. With $d_{\text{LC}} = 4.8$ μm, $A = 25$ mm^2, $\gamma = 0.04$ kg/s m, and $P = 850$ nC/cm^2, we obtain $R_{P \min} = \gamma d_{\text{LC}} / A P^2 = 106$ Ω. The corresponding effective minimum bulk resistivity of the LC during polarization reversal is $\rho_{P \min} = A R_{P \min} / d_{\text{LC}} = 5.5 \times 10^4$ Ω cm, a value that is in the semiconducting range. That is, because of the
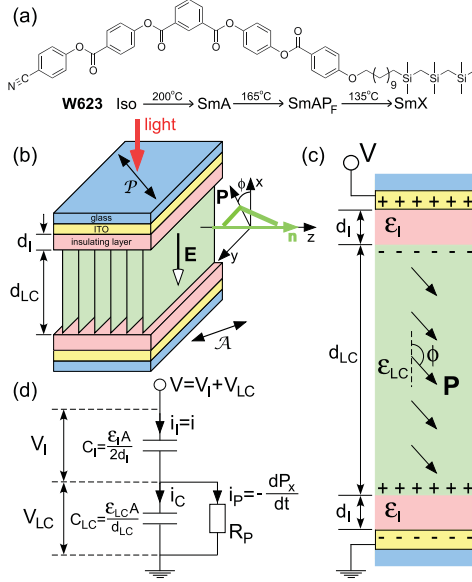
_____

*Noel.Clark@Colorado.Edu

FIG. 1. (Color online) Block polarization reorientation in a fluid, polar liquid crystal. (a) Chemical structure and phase sequence on cooling of W623. (b) Electro-optic geometry, showing a bent-core molecule in the $\text{Sm}AP_F$ phase in a bookshelf cell with ITO electrodes and rubbed polyimide insulating layers. The director $\mathbf{n}$ is along the layer normal $\mathbf{z}$, independent of applied field $\mathbf{E}$. The polarization $\mathbf{P}$ is normal to the director and makes an angle ϕ relative to the cell normal $\mathbf{x}$. An analog electro-optic response is observed with normally incident light and the cell between the crossed polarizer and analyzer. (c) Model of electrostatically controlled block polarization reorientation, showing liquid crystal and polyimide insulating layers, with thickness d and dielectric constant ϵ, and ITO electrodes. When the applied voltage $|V| < V_{\text{sat}} = 2d_I P/\epsilon_I$, the polarization $\mathbf{P}$ reorients as a homogeneous block to exclude the electric field from the liquid crystal. (d) Equivalent circuit of the cell under time-varying applied voltage $V(t)$.

large value of P, the effective resistivity during reorientation is much smaller than the intrinsic static LC resistivity ($\rho_{\text{LC}} \sim 10^{12}$ Ω cm). As $\mathbf{P}$ approaches alignment with the applied field ($\phi = 0$ or π), $P_x^2(\phi)$ approaches P_2 and $R_P(\phi)$ increases, diverging to infinity in these limits.

The key experimental probe of R_P is the variation of the cell current $i(t)$ accompanying the analog reorientation of $\mathbf{P}$, particularly the flat-topped step found in response to a triangle wave $V(t)$ shown in Figs. 2(a) and 2(b). This feature was noted previously in high-P LC cells with insulating layers, but was not quantitatively interpreted [11]. We show below that this plateau is a universal signature of the temporal dependence of R_P that should be expected for fluid smectics with substantial polarization ($P \gtrsim 300$ nC/cm^2) undergoing block polarization reorientation in cells with insulating layers on the electrodes.

The overall electrical response of the LC cell depends on its effective RC time constant. For a typical cell with $C_{\text{LC}} \sim 1$ nF and $C_I \sim 10$ nF, the minimum $\tau_{\text{LC min}} = R_{P\,\text{min}} C_{\text{LC}}$ is on the order of 10^{-7} s and $\tau_{I\,\text{min}} = R_{P\,\text{min}} C_I \sim 10^{-8}$ s. Such short time constants imply that the polarization current will effectively short out the liquid crystal capacitance C_{LC} for typical millisecond to microsecond LC reorientation

processes, the cell appearing electrically as C_I in series with R_P. As a result, if the time in an ac cycle during which $\mathbf{P}$ rotates between $\phi = 0$ and π is large compared to τ_{LC}, then the cell response is dominated by the insulating layers and the cell appears to be capacitive, with impedance $Z_I \approx (j\omega C_I)^{-1}$. However, as ϕ approaches 0 or π, P_x saturates, R_P diverges to infinity, and the cell impedance becomes $Z_{\text{sat}} = (j\omega C_I)^{-1} + (j\omega C_{\text{LC}})^{-1} \approx (j\omega C_{\text{LC}})^{-1}$. Since $\tau_{\text{LC min}}$ is typically very small, this crossover from small to large R_P behavior occurs very near the limiting orientations $\phi = 0$ and π. The ratio of the cell impedances before and after saturation is $Z_I/Z_{\text{sat}} \approx C_{\text{LC}}/C_I$. The corresponding current jumps by an amount I, from $C_I(dV/dt)$ for $|V| < V_{\text{sat}}$ to $C_{\text{LC}}(dV/dt)$ for $|V| > V_{\text{sat}}$, giving a characteristic plateau. As R_P transitions from $R_P \sim 0$ to ∞, V_{LC} changes from $V_{\text{LC}} \sim 0$ to $V(t) \pm V_{\text{sat}}$, where the plus sign applies when $V > 0$. Ion conduction is therefore only significant when $|V| > V_{\text{sat}}$.

In our experiments, the cell is placed between crossed polarizers and illuminated at normal incidence by a He-Ne laser beam with wavelength $\lambda = 632$ nm. The transmitted intensity is given by $T = T_\circ \sin^2 2\psi \sin^2(\pi \Delta n d/\lambda)$, where ψ is the angle between the analyzer and the optic axis of the liquid crystal and d is the cell thickness. In high polarization chiral SmC materials, the optic axis orientation is coupled to the direction of $\mathbf{P}$, with the director moving on the tilt cone in an applied field and giving contrast in the optical transmission. In the SmAP_F case, the molecular long axis remains along the layer normal $\mathbf{z}$ as $\mathbf{P}$ reorients [4,12]. The phase is, however, strongly biaxial, with n_p, the refractive index along $\mathbf{P}$, larger than $n_\circ$, the index normal to the bow plane, so that in the geometry of Fig. 1(b), the effective birefringence Δn changes from $\Delta n = n_z - n_p$, when there is no applied field and $\mathbf{P}$ is parallel to the glass, to $\Delta n = n_z - n_\circ$, at high applied electric field, where $\mathbf{P}$ is aligned normal to the glass [4,7]. The birefringence can be modulated with an applied electric field to control the optical transmission. For example, at low temperature ($T = 140\,^\circ\text{C}$) the effective birefringence of W623 changes substantially with applied field, from $\Delta n(E = 0) \approx 0.09$ to $\Delta n(E = 10$ V/μm$) \approx 0.115$.

The current and optical response when the SmAP_F cell is driven by a 10-Hz triangular voltage is shown in Fig. 2(a). When the applied voltage $|V| < V_{\text{sat}}$, $\mathbf{P}$ rotates between $\phi = 0$ and π and the transmission curve is V shaped due to the analog change in birefringence. As analyzed above, in this regime, the polarization effectively short circuits the LC and the current is constant, the current response curve showing a flat-topped peak with magnitude $I \approx C_I|dV/dt|$. When the sign of the slope of the applied voltage changes, the current jumps by an amount $I' = [2C_I C_{\text{LC}}/(C_I + C_{\text{LC}})]|dV/dt|$. The spontaneous polarization of the SmAP_F phase increases on cooling as a result of reduced thermal fluctuations in the orientation angle ϕ, reaching a maximum value of 850 nC/cm^2 just above the transition to the SmX phase. Since $V_{\text{sat}} = 2d_I P/\epsilon_I$, the larger the polarization, the higher the voltage required to achieve saturation and the broader the current peak, as illustrated in Fig. 2(b). The height of the peak does not change. The saturation voltage V_{sat} at different temperatures, shown in Fig. 2(c), is found to be proportional to polarization, as predicted, with a fit giving $d_I/\epsilon_I = 0.008\,50$ V/(nC/cm^2).
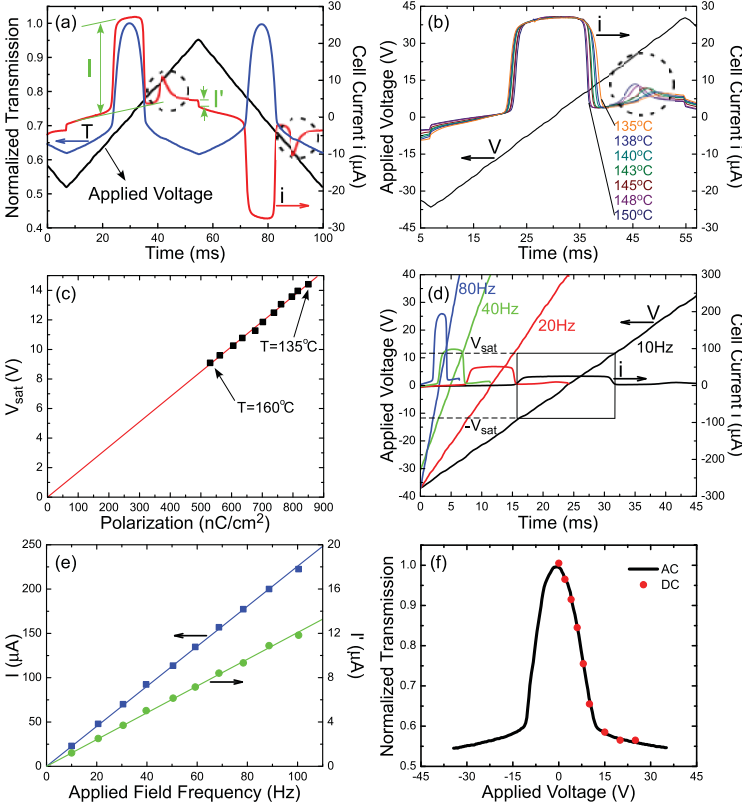
FIG. 2. (Color online) Experimental measurements of electro-optic and current response of W623 in a 4.8-μm-thick cell with ITO electrodes and rubbed polyimide alignment layers. (a) Electro-optic response with the layer normal oriented at 45° to crossed polarizers ($T = 158\,°C$). The current through the cell i in the analog reorienting regime has a constant magnitude I, i.e., the cell is capacitive, with the liquid crystal polarization acting effectively as a local short circuit. I' is the magnitude of the current step when the slope of the applied voltage changes. The background slope of the total current arises from the finite cell resistance. The triangular applied voltage V varies between ±40 V. (b) Current i at different temperatures with a triangular voltage applied to the cell. The current peaks due to ions are circled in (a) and (b). (c) Saturation applied voltage measured as a function of spontaneous polarization. The red line is a fit. (d) Current i vs time for triangular applied voltages with different driving frequencies ($T = 145\,°C$). In all cases, polarization current flows when $|V| < V_{\text{sat}}$, as illustrated by the box highlighting the 10-Hz data. (e) I and I' measured as a function of the frequency of the applied triangular voltage ($T = 145\,°C$). The lines are best fits. (f) Optical transmission in ac (50-Hz triangular voltage) (solid line) and dc (symbols) applied fields ($T = 145\,°C$). The transmitted light intensity level with an applied dc voltage remains constant for at least one hour.

The current peaks due to ion transport in the LC occur shortly after $|V|$ exceeds V_{sat}, immediately following the polarization current peaks, and are circled in Figs. 2(a) and 2(b). There is no ion current in the low voltage, analog regime because $E_{\text{LC}} \approx 0$ for $|V| < V_{\text{sat}}$.

Since the LC cell is capacitive during polarization reorientation, the height of the flat peak increases with driving frequency, as illustrated in Fig. 2(d). The saturation voltage V_{sat} is, however, independent of frequency at a given temperature. To explore the relationship between I, I', and $|dV/dt|$ we measured the current response at fixed temperature while applying a triangular voltage with constant amplitude ($V_{\text{max}} = 38.47$ V) and variable frequency to the cell. As shown in Fig. 2(e), I and I' depend linearly on f as expected, with slopes 2.26 and 0.12 μA/Hz, respectively. Since $|dV/dt| = 4V_{\text{max}}f$, we have $4V_{\text{max}}C_I = 2.26$ μA/Hz and $4V_{\text{max}}[2C_I C_{\text{LC}}/(C_I + C_{\text{LC}})] = 0.12$ μA/Hz, which we can solve to find $C_I = 14.69$ nF and $C_{\text{LC}} = 0.40$ nF. Since $C_I = \epsilon_I A/2d_I$ and $C_{\text{LC}} = \epsilon_{\text{LC}}A/d_{\text{LC}}$, taking $\epsilon_I = 3.5\epsilon_\circ$ (for polyimide), $d_{\text{LC}} = 4.8$ μm, and $A = 25$ mm^2, we obtain $d_I = 26.4$ nm and $\epsilon_{\text{LC}} = 8.7\epsilon_\circ$. We may then compute $d_I/\epsilon_I = 0.008\,51$ V/(nC/cm^2), which agrees with the value obtained above from the slope of the saturation voltage vs polarization curve.

The dynamics of block polarization reorientation in a time-varying electric field may be modeled by finding simultaneously the polarization orientation ϕ, the current through the cell i, and the electric field in the liquid crystal E_{LC}. The effect of ions is discussed separately. Referring to the equivalent circuit shown in Fig. 1(d) and using $i_I = C_I dV_I/dt$, $i_C = C_{\text{LC}}dV_{\text{LC}}/dt$, and Eqs. (1) and (2), we may write down the following expressions that are valid in the analog regime

when $|V| < V_{\text{sat}}$:

$$\frac{d\phi}{dt} = \frac{1}{\tau_\circ}\left(\frac{V}{V_{\text{sat}}} + \cos\phi\right)\sin\phi, \qquad (3)$$

$$i = C_I \frac{dV}{dt} - C_I \frac{\gamma d_{\text{LC}}}{P}\frac{d}{dt}\left(\frac{1}{\sin\phi}\frac{d\phi}{dt}\right), \qquad (4)$$

$$E_{\text{LC}} = \frac{\gamma}{P\sin\phi}\frac{d\phi}{dt}. \qquad (5)$$

Here $V_{\text{sat}} = 2d_I P/\epsilon_I$ is the saturation voltage and $\tau_\circ = (1 + C_{\text{LC}}/C_I)\gamma d_{\text{LC}}/PV_{\text{sat}}$ is the time constant for director reorientation near $V = 0$ (where $\phi = \pi/2$) [8]. When $|V| > V_{\text{sat}}$, ϕ is aligned along $\phi = 0$ or π, $d\phi/dt = 0$, and the current from the reorientation of the spontaneous polarization vanishes, yielding

$$i = \frac{C_I C_{\text{LC}}}{C_I + C_{\text{LC}}}\frac{dV}{dt}, \qquad (6)$$

$$E_{\text{LC}} = \frac{C_I}{C_I + C_{\text{LC}}}\frac{V \pm V_{\text{sat}}}{d_{\text{LC}}}. \qquad (7)$$

Numerical solutions of Eqs. (3)–(7) are plotted in Fig. 3. Using the cell parameters obtained above and assuming $P = 850$ nC/cm^2, we have $V_{\text{sat}} = 14.7$ V and $\tau_\circ = 1.6 \times 10^{-6}$ s. A 10-Hz triangular voltage with $V_{\text{max}} = 2V_{\text{sat}}$, shown in Fig. 3(a), is applied to the model cell. Figure 3(b) shows the reorientation of the polarization field between $\phi = 0$ and π when $|V| < V_{\text{sat}}$ and the corresponding optical transmission of the cell. Since the time constant $\tau_\circ \propto P^{-2}$ and P is large,
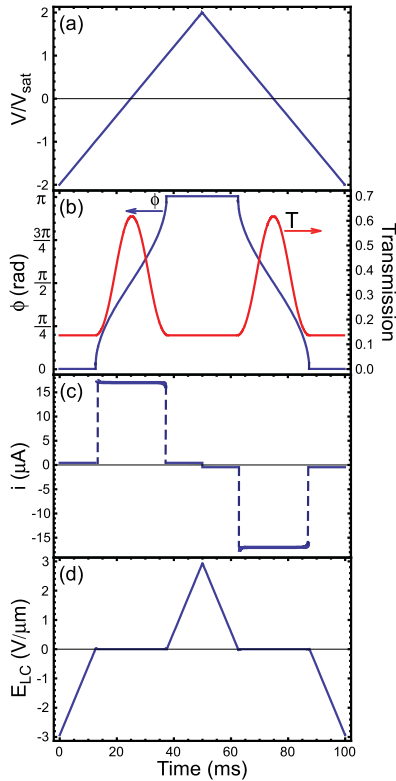
FIG. 3. (Color online) Simulated electro-optic response of a polar Sm*A* bent-core liquid crystal cell driven by a 10-Hz triangular voltage with $V_{max} = 2V_{sat}$. The cell parameters are given in the text. (a) Applied voltage. (b) Polarization orientation and optical transmission. (c) Polarization current. (d) Electric field in the liquid crystal. In the analog regime, the internal field is small but nonzero for finite driving frequencies.

$\tau_\circ$ is small compared with the period of the driving voltage and ϕ quickly relaxes to its static value. Since $\gamma d_{LC}/P \approx 2.3 \times 10^{-5}$ V s $\ll 1$ V s, the second term in Eq. (4) is small compared to the first, so that $i \approx C_I(dV/dt)$. In other words, the cell looks capacitive when $|V| < V_{sat}$, as though only the insulating layers were present, and the polarization current associated with block polarization reorientation is constant. Since the saturation voltage $V_{sat} \propto P$, V_{sat} is large and there is a broad, flat-topped peak in the i vs time curve in Fig. 3(c). If a static voltage $|V| < V_{sat}$ is applied to the cell, the polarization reorients as a block to screen the electric field in the liquid crystal E_{LC} completely. However, if the applied

voltage varies in time, as in the present experiments, E_{LC} is small but nonzero ($\sim 10^{-4}$ V/μm). Once the orientation of **P** has saturated (when $|V| \geqslant V_{sat}$), E_{LC} increases linearly with voltage as $E_{LC} \approx (V \pm V_{sat})/d_{LC}$ [Fig. 3(d)], inducing ion flow in the LC cell.

If the resistance of the insulating layers is sufficiently high, the absence of an electric field in the LC layer when $|V| < V_{sat}$ leads to an analog electro-optic response to dc or quasistatic applied voltage that is free of ion screening effects over long times. This is demonstrated in Fig. 2(f), where we compare the W623 cell transmission using a 50-Hz triangle wave applied voltage to that obtained after applying dc voltage for one hour. The transmission for dc voltages matches the dynamic response at the same voltage and shows little change over time.

At $V = 0$, **P** relaxes slowly to $\phi = \pi/2$, due to an effective field $E_s \approx W_\circ/P d_{LC}$ in the LC arising from surface anchoring, where $W_\circ$ is the Rapini-Papoular surface anchoring energy. Taking $W_\circ = 2 \times 10^{-7}$ J/m^2, $P = 750$ nC/cm^2, and $d_{LC} = 4.8$ μm, we obtain $E_s \approx 5 \times 10^{-6}$ V/μm. This field will transport ions in the cell through the LC layer, replacing polarization charge and thus allowing **P** to relax back to its surface-preferred orientation at $\phi = 0$. The ion current peaks observed for $|V| > V_{sat}$ enable an estimate of the field-induced ion transit time t_{ion} in the LC. In Fig. 2(a), the first ion current peak occurs when $E_{LC} \approx 2$ V/μm and has a duration of about 5 ms, from which we estimate $t_{ion} \approx 10$ ms [13]. By assuming $t_{ion} \propto 1/E$ and taking $E = E_s$, the corresponding orientation relaxation time in a static applied voltage under the action of the surface is $t_{ion} \approx 1$ h, although this should be considered a lower limit since charge screening will reduce the current at low field.

In summary, an electric field applied to bent-core liquid crystals causes reorientation of the spontaneous polarization with a characteristic current response. Analysis of the dynamics of the director response to a time-dependent applied voltage shows that the effective resistivity drops into the semiconducting range during reorientation. This behavior is confirmed experimentally in the biaxial SmAP_F phase of W623, where block reorientation of the director enables a simple mode of analog control of birefringence.

[1] M. E. Lines and A. M. Glass, *Principles and Applications of Ferroelectrics and Related Materials* (Oxford University Press, New York, 2001).
[2] R. B. Meyer *et al.*, J. Phys. Lett. **36**, 69 (1975).
[3] D. M. Walba *et al.*, Science **288**, 2181 (2000).
[4] R. A. Reddy *et al.*, Science **332**, 72 (2011).
[5] R. Pindak, C. Y. Young, R. B. Meyer, and N. A. Clark, Phys. Rev. Lett. **45**, 1193 (1980).

[6] D. Coleman *et al.*, Phys. Rev. Lett. **91**, 175505 (2003).
[7] M. J. O'Callaghan *et al.*, Appl. Phys. Lett. **85**, 6344 (2004).
[8] M. J. O'Callaghan, Phys. Rev. E **67**, 011710 (2003).
[9] A. Hammarquist *et al.*, Phys. Rev. E **77**, 031707 (2008).
[10] N. A. Clark *et al.*, Mol. Cryst. Liq. Cryst. **94**, 213 (1983).
[11] A. D. L. Chandani *et al.*, Liq. Cryst. **26**, 167 (1999).
[12] H. R. Brand *et al.*, Macromolecules **25**, 7223 (1992).
[13] Z. Zou *et al.*, Ferroelectrics **121**, 147 (1991).